Colloid Polym Sci (2006) 285:263–272
DOI 10.1007/s00396-006-1559-7

ORIGINAL CONTRIBUTION

Effect of the crosslinking density and the method of sample preparation on the observed microstructure of macroporous and conventional poly(*N*,*N*-dimethylacrylamide) hydrogels

Isabel E. Pacios · Alejandra Pastoriza · Ines F. Pierola

Received: 23 June 2006 / Accepted: 28 July 2006 / Published online: 10 October 2006

Abstract SEM micrographs of macroporous and conventional poly(*N*, *N*-dimethylacrylamide) hydrogels were obtained for specimens synthesized in different conditions and prepared for microscopy by different methods (freeze drying of different solvents and critical point drying). The crosslinking density of both types of samples was determined through T_g measurements. Open structures (honeycomb-like, fibrillar networks) were more frequently observed in specimens prepared by freeze drying of benzene, which was attributed to its large pressure and temperature at the triple point. In spite of the different structure in the millimeter scale, there is no significant difference in the mesh size of fibrillar networks observed for macroporous and conventional samples, and in both cases it decreases with increasing crosslinking density. Other effects of the crosslinking density are that only incomplete honeycomb-like structures were formed in low-crosslinking samples and that collapsed structures were developed by phase separation throughout polymerization in highly crosslinked samples. Fibrillar networks of 1-μm mesh size were observed for the uncrosslinked polymer.

Keywords Crosslinking · Microstructure · Macroporous · Poly(*N*, *N*-dimethylacrylamide) · Hydrogels

Introduction

Swelling properties of hydrogels, at equilibrium or in their time evolution, are frequently correlated with the polymer structure in the micrometer scale measured by SEM. Within that context, many different microstructures were reported [1–8]. Some studies consider the dependence of the hydrogel morphology on variables such as the size of the filler particles [1], the polymer composition [2], the swelling solvent [3, 4], the method of preparing the specimen for SEM [5], or the previous treatment of the sample [6]. The objective of this work is to gain a better understanding of the relationship of the conditions of synthesis and sample preparation, with the microstructure of hydrogels, and with that purpose we have chosen crosslinked poly(*N*, *N*-dimethylacrylamide) (PDMAA), a hydrogel of well known characteristics [7, 8].

Several methods of preparing the specimens for SEM observations were reported. This technique requires solid samples, which are attained by freeze-etching [5] or drying the swollen hydrogel in conditions such that the structure of the polymer matrix is preserved in the solid state as close as possible to that in the swollen state. The most frequent methods employed for drying were: air or vacuum drying under melting conditions [9], lyophilization or freeze drying of water swollen samples [10], and critical point drying of samples swollen with supercritical CO_2 [5, 8]. Environmental SEM (ESEM) [3, 11] does not require solid samples because it may give good micrographs of water swollen samples without an electrically conducting coat. Other techniques based in SEM were also employed to investigate the microstructure of hydrogels and biological macromolecules [12–14].

These different methods yield different observed microstructures. The specimens dried under frozen conditions yield good images of the polymer matrix as it is in the swollen state (open structures). Nevertheless, if, for some accidental reason, the solvent melts during drying, the polymer mobility becomes enough to reaccommodate to the

I. E. Pacios · A. Pastoriza · I. F. Pierola (✉)
Departamento de Ciencias y Técnicas Fisicoquímicas,
Facultad de Ciencias, Universidad a Distancia (UNED),
28040 Madrid, Spain
e-mail: ipierola@ccia.uned.es

decreasing solvent proportion in-between chains and the pores collapse [9, 10], giving place to compact structures coexisting with open structures observed in nonmelting zones. It must also be taken into account that, in some cases, samples undergo phase separation throughout polymerization in such a way that they are intrinsically formed only by collapsed structures [15, 16]. The surface and the bulk of the specimen are frequently different in microstructure and not only because of the method of preparation [9].

Macroporous hydrogels have porous structure in the millimeter to the hundred-micrometer scale [7, 8], which is responsible for the large swelling capacity and fast response to external stimuli of these materials [7]. In this work we aim to compare the structure of macroporous and conventional hydrogels in a length scale below the size of macropores and to observe the influence of the crosslinking density on that microstructure.

Experimental

Synthesis

Conventional samples of PDMAA hydrogel (h-PDMAA) were synthesized by radical crosslinking polymerization of *N*,*N*-dimethylacrylamide (Aldrich) and *N*,*N*′-methylene-bis-acrylamide (Fluka) (BA) in aqueous solution, with 4.8 to 4.9 M total comonomer concentration (C_T) and different crosslinker ratios (*C*, percent moles of BA with respect to moles of DMAA). The redox pair potassium persulfate/triethanolamine (Probus/Carlo Erba) at 1.8×10^{-3}-M concentration was employed as initiator at room temperature. Water was deionized with the Milli-Q system from Millipore. The feeding mixture was deaerated by sonication. Gelation took place within 5 min, and afterwards, samples were kept at 6 °C for 3 days to complete reaction.

Macroporous samples (mh-PDMAA) were synthesized [7] with the same components in bulk, with 9.7 to 9.9 M C_T and several *C*, at 80 °C until gelation (5 to 15 min) and at room temperature later (6 days) to complete the polymerization. Since the boiling point of the feeding is about 80 °C, once at that temperature, the system generated numerous unconnected small bubbles, which were trapped during gelation and resulted in holes of about 1 mm in diameter, homogeneously distributed in the final samples.

Once the polymerization was finished, the hydrogels were taken out of the molds, cut as disk-like pellets, and washed by immersion in a large excess of water for several weeks. Washing water was replaced frequently until volume changes were no longer observed. Hereafter, crosslinked samples are labeled as h- or mh-PDMAA(C_T)*C*. For example, h-PDMAA(4.8)0.24 represents a conventional hydrogel obtained with 4.8 M total comonomer concentration in the aqueous solution and a comonomer mixture having 0.24% mole BA with respect to moles of DMAA.

Linear (uncrosslinked) PDMAA (l-PDMAA) was also prepared by radical polymerization in aqueous solution with 0.80 M monomer concentration at 65 °C with azobis-isobutyronitrile 1.1×10^{-3} M as initiator [17]. After 20 h of reaction, it was precipitated over cold acetone (in a volume such that the final composition was 90/10 acetone/water) and dried in open air. Its intrinsic viscosity was measured in a Lauda Viscometer, in methanol solution, at 25 °C, leading [18] to a molecular weight $M_v = 3 \times 10^6 g/mol$. This linear sample was soluble in water and many organic solvents (tetrahydrofuran, dimethylformamide, acetone...), but in benzene it only swelled without achieving dissolution, and this peculiarity was used in sample preparation for SEM measurements: l-PDMAA swollen in benzene was freeze dried.

Measurements

Scanning electron microscopy (SEM) measurements were carried out in a JEOL JSM 6400 electron microscope. Three different methods were employed for preparation of the solid specimens: (1) freeze drying of samples swollen in benzene, (2) freeze drying of samples swollen in water, and (3) critical point drying of samples swollen in supercritical CO_2 using a Balzers SCD 030 critical point dryer. Swelling in benzene or supercritical CO_2 was preceded by a slow and progressive exchange of swelling water by acetone and later of acetone by benzene or supercritical CO_2. In all cases, solid specimens were coated with gold by means of a Balzers SCD 004 sputter-coater. Surface and bulk structures were observed. Inner parts of the specimens were revealed by simply cutting them with a bistoury or by cryogenic fracture. Several specimens of each sample were studied and several micrographs of any relevant portion were taken for each specimen.

Analysis of the SEM micrographs was performed with the public-domain ImageJ program [19]. A threshold procedure was applied to the digitalized images and the validity of the threshold procedure was confirmed by comparing the images before and after the procedure. After calibrating with a known scale, the program measures the Feret's diameter of each dark region, which in the micrograph corresponds to a micropore between polymer walls or filaments. The Feret's diameter, also known as the caliper length, represents the longest distance between any two points along the selection boundary, i.e., the mesh size of the polymer network.

The thermal analysis was carried out by means of a Mettler Toledo 12E differential scanning calorimeter (DSC) provided with a DSC822 oven and a subambient cooling

unit. The temperature response of the calorimeter was calibrated with the melting points of high-purity samples of zinc and indium. Reproducibility of temperature readings, from single thermograms of any calibrating sample, was below ±0.2%. At least two DSC experiments were made for each sample with xerogel specimens of 8 and 10 mg, determined within ±0.02 mg by means of a Mettler Toledo AG285 electrobalance. Two runs were performed with each specimen, in a nitrogen atmosphere, using an empty aluminum cell as a reference. Both were scanned at 10 °C/min in the range 30–240 °C. Only second-run results are presented. Among the several criteria proposed for the determination of Tg, we selected the inflection point obtained with the software of the instrument. Glass transition temperatures from independent thermograms were reproducible to better than 0.4 °C. Heat capacity values, from two or three independent runs, were within 2–3% of any single value.

Results and discussion

Crosslinked PDMAA samples were synthesized with several total comonomer concentrations and crosslinker ratios in the reacting mixture (Table 1) and at two different temperatures: room temperature and the boiling point of the reacting mixture, about 80 °C. During gelation of samples prepared at the higher temperature, the bubbles of the boiling system were trapped in positions homogeneously distributed, and thereafter, postgel reactions fixed them. These samples were macroporous, showing about three times the swelling capacity of conventional hydrogels synthesized at room temperature with the same reacting mixture composition [7]. Macroporous mh-PDMAA hydrogels thus obtained were transparent with plenty of visible holes, except for sample mh-PDMAA(9.9)2.3, which was opaque. Conventional h-PDMAA hydrogels, prepared at room temperature, were transparent. Once we determined the crosslinking density of all these samples, we studied their microstructure by SEM.

Crosslinking density

Crosslinked polymers are usually characterized by means of the effective crosslinking density (ν_e) or number of elastically effective chains per unit volume of xerogel. It is often determined through swelling measurements with the Flory–Rehner equation [20]. Such equation may not be applied to macroporous hydrogels because water retained in macropores behaves as external water rather than as water swelling the polymer network. Such external water significantly increases swelling with respect to the conventional samples of the same feeding composition [7] without modifying the mixing and elastic contributions to the osmotic pressure, and thus, artifactual ν_e values are obtained for mh-PDMAA through swelling measurements. On the other hand, compression and dynamic mechanical analysis also allow to determine crosslinking densities, but in this case, the lack of mechanical integrity of some of the samples and the foam-like structure of others were inadequate for mechanical measurements.

An alternative method to determine ν_e is via measurement of the glass transition temperature because permanent crosslinks limit chain mobility, causing an increment of T_g [21, 22]. DSC measurements are appropriated for the samples here studied because they require powdered specimens and sense only the nanometer scale. The thermograms of PDMAA xerogels show the pattern depicted in Fig. 1, a glass transition whose T_g increases upon increasing the crosslinker ratio in the polymerization mixture and whose heat capacity jump (ΔC_p) remains practically constant (Table 1). The glass transition becomes broader with

Table 1 Temperature and heat capacity jump of the glass transition of conventional and macroporous PDMAA hydrogels synthesized with different concentrations of bifunctional monomer (DMAA) and crosslinker (BA)

Sample	[DMAA] (mol/L)	[BA] (mol/L)	T_g (°C)	ΔC_p (J/gK)
l-PDMAA	0.80	0	125.6	0.28
h-PDMAA(4.8)0.24	4.84	0.0118	127.1	0.28
h-PDMAA(4.9)0.47	4.89	0.0232	128.9	0.28
h-PDMAA(4.9)0.52	4.84	0.0250	129.2	0.29
h-PDMAA(4.9)0.58	4.86	0.0281	129.7	0.30
h-PDMAA(4.9)1.0	4.84	0.0484	131.4	0.30
h-PDMAA(3.0)0.92	2.97	0.0273	132.9	0.30
mh-PDMAA(9.7)0.26	9.70	0.0251	128.2	0.30
mh-PDMAA(9.7)0.36	9.70	0.0347	128.6	0.28
mh-PDMAA(9.8)0.62	9.70	0.0598	129.5	0.29
mh-PDMAA(9.9)2.3	9.70	0.2260	135.2	0.27

Data for l-PDMAA are also included

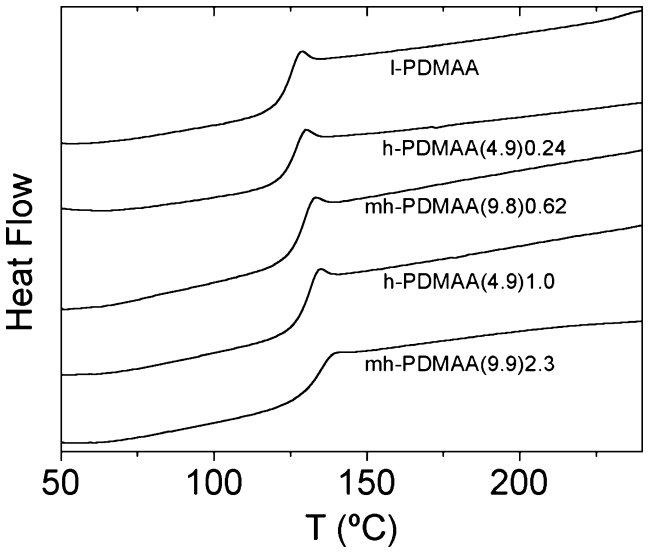

Fig. 1 Second run DSC profile of **a** uncrosslinked PDMAA and PDMAA xerogels: **b** h-PDMAA(4.8)0.24; **c** mh-PDMAA(9.8)0.62; **d** h-PDMAA(4.9)1.0; **e** mh-PDMAA(9.9)2.3

increasing ν_e, as observed for other similar polymers [22, 23].

In the frame of the Gibbs–DiMarzio theory of glass transitions, the following expression was derived [24] relating T_g with ν_e, the permanent crosslinking density

$$T_g - T_g^L = T_g^L \frac{kM_O\nu_e/\rho_2\gamma}{1 - kM_O\nu_e/\rho_2\gamma} \quad (1)$$

where T_g^L stands for the glass transition temperature of uncrosslinked polymer (125.6 °C), k is a parameter about independent of the polymer and equal to 1.3×10^{-23} in molecular units, M_o is the molecular weight of the polymer repeating unit, ρ_2 is the xerogel density (1.06 g/cm^3), and γ is the number of flexible bonds per monomeric unit (three for acrylic polymers as PDMAA [24]). The experimental error in the determination of ν_e depends on the shift of T_g with respect to that of the uncrosslinked polymer. The smallest shift here observed is 1.5 °C (see Table 1) with ±0.4 °C experimental error, and therefore, the uncertainty of the minimum crosslinking density is about 30%, which was taken into account in the size of symbols in Fig. 2. That represents the worse situation. The largest shift is 10.4±0.4 °C (see Table 1) and, correspondingly, the uncertainty of the maximum crosslinking density in Fig. 2 is about 4%.

Figure 2 shows that ν_e values obtained with Eq. (1) increase with the crosslinker ratio in the reacting mixture. They remain below ν_e(IN), the crosslinking density corresponding to an ideal network

$$\nu_e(IN) = \frac{2\rho_2[BA]}{C_T M_O} \quad (2)$$

owing to the consumption of BA molecules in network defects [22, 25]. Points corresponding both to conventional and macroporous samples fall into a single master curve, indicating that the structure at the nanometric scale was not affected by differences in the method of synthesis or by the existence of macropores in the millimeter scale.

Image processing

SEM micrographs of PDMAA hydrogels show several repeated structures that may be classified as open and collapsed microstructures. Figures 3, 4, and 5 illustrate the three observed open structures: fibrillar networks (FN) [26], honeycomb-like networks (HC) [27], and intermedium structures formed by broken interconnected films (BIF). In FN structures, polymer spheres [8] join in filaments to form a continuous three-dimensional network, with empty and totally interconnected holes isotropically distributed (Fig. 3). In BIF structures, primary polymer spheres are, in part, connected in filaments, but the polymer also forms part of short pieces of thin films (Fig. 4). In HC structures, polymer films form the walls of elongated cells with about hexagonal section, noninterconnected, and oriented parallel to each other as in a pipe organ (Fig. 5).

Each micrograph was analyzed with ImageJ software [19], which allows determining the frequency distribution of Feret's diameters of empty spaces between polymer filaments of FN structures as much as between polymer films of HC or BIF structures. Figure 6 shows some representative examples of Feret's diameter frequency distributions of FN structures. The mean Feret's diameter (D) and the width of the distribution (ΔD) characterize a distribution, i.e., the microstructure observed in each

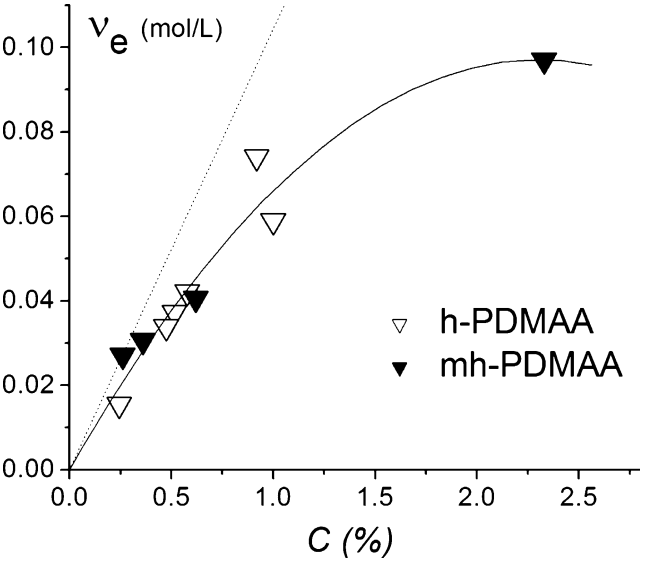

Fig. 2 Crosslinking density of macroporous and conventional PDMAA hydrogels synthesized with different crosslinker ratios. The *solid line* corresponds to the second order polynomial fit to all the points and the *dotted line* to the crosslinking density following from stoichiometry in a perfect network

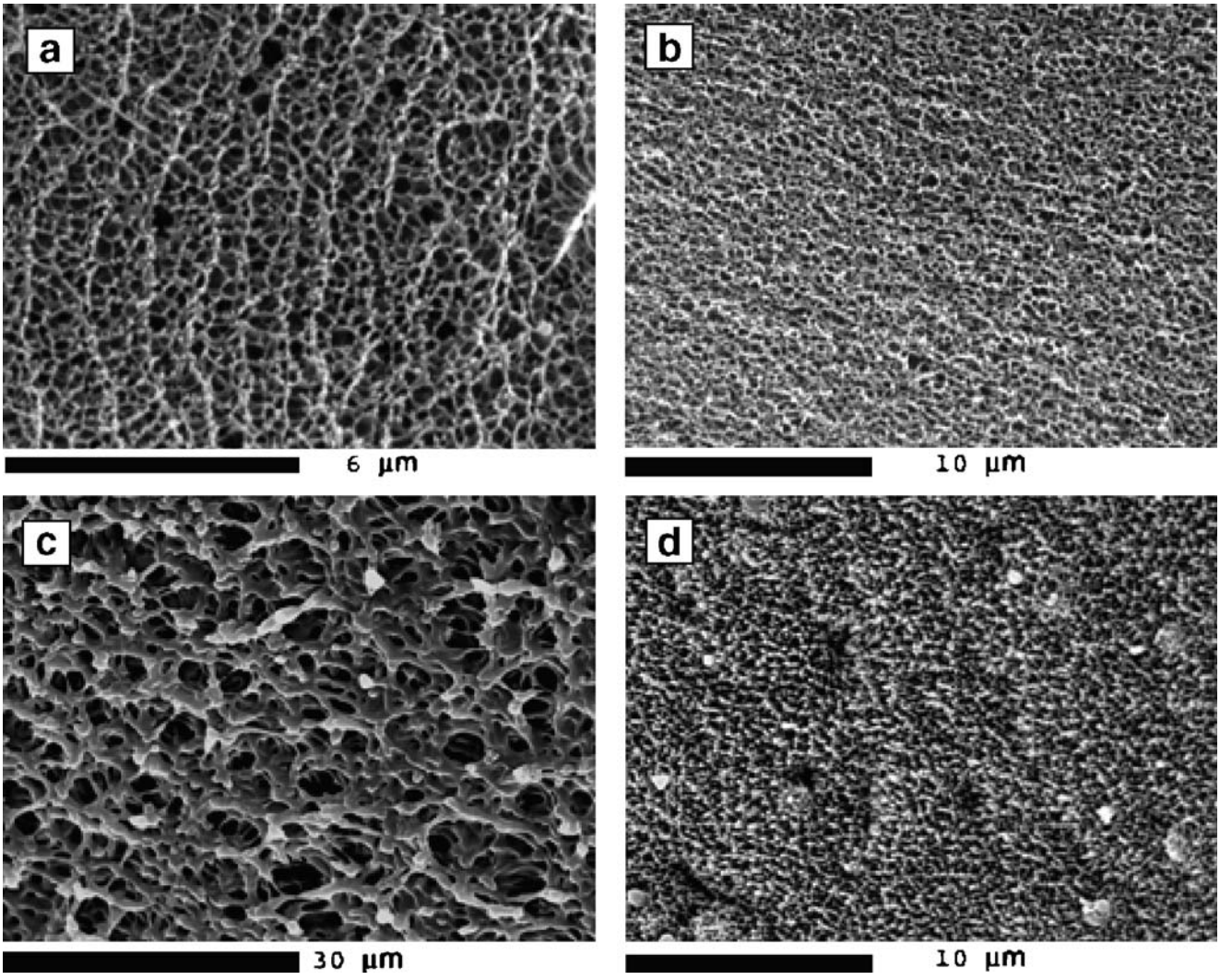

Fig. 3 SEM micrographs of several FNs observed on samples freeze dried from benzene: **a** h-PDMAA(4.8)0.24; **b** h-PDMAA(4.9)0.52; **c** l-PDMAA; **d** mh-PDMAA(9.8)0.62

micrograph. Such information is restricted to the zone focused in the micrograph and it might not be representative of the whole sample. For that reason, D and ΔD were determined for a large number of micrographs of each sample (all them showing the same type of microstructure), and the average values (D_{av}, ΔD_{av}) appear summarized in Table 2. Interestingly, it was found for some hydrogels that this type of analysis of SEM micrographs yields pore size ranges in close agreement with those determined by mercury intrusion porosimetry [28].

Size of the open microstructures

FN structures (Fig. 3a–d) were found in practically all the samples studied here: uncrosslinked polymer and macroporous and conventional gels. Two aspects of the observed FN mesh size are remarkable; on one side, Fig. 7 shows that for each sample (each crosslinking density) a broad range of mean Feret's diameters were obtained in the different micrographs, but in spite of the large size heterogeneity of any sample, the trend seems to descend with increasing ν_e. On the other side, within the range of dispersion of D values, it can be said that both macroporous and conventional gels show in Fig. 7 the same behavior, and the average diameter or mesh size (Table 2) is around 0.3 μm for all the gels. Linear PDMAA also shows a FN microstructure (Fig. 3c), but in this case the mesh size is larger, above 1 μm (Table 2).

Polymer filaments are much thicker for linear (around 1 μm) than for crosslinked samples (around 0.07 μm), as determined on the micrographs of the largest magnification. These filament thicknesses are larger than the radius of gyration (R_g) expected for chains between crosslinks, in the case of hydrogels, and for coils of uncrosslinked PDMAA. For example, for h-PDMAA(4.8)0.24, the molecular weight of chains between crosslinks is

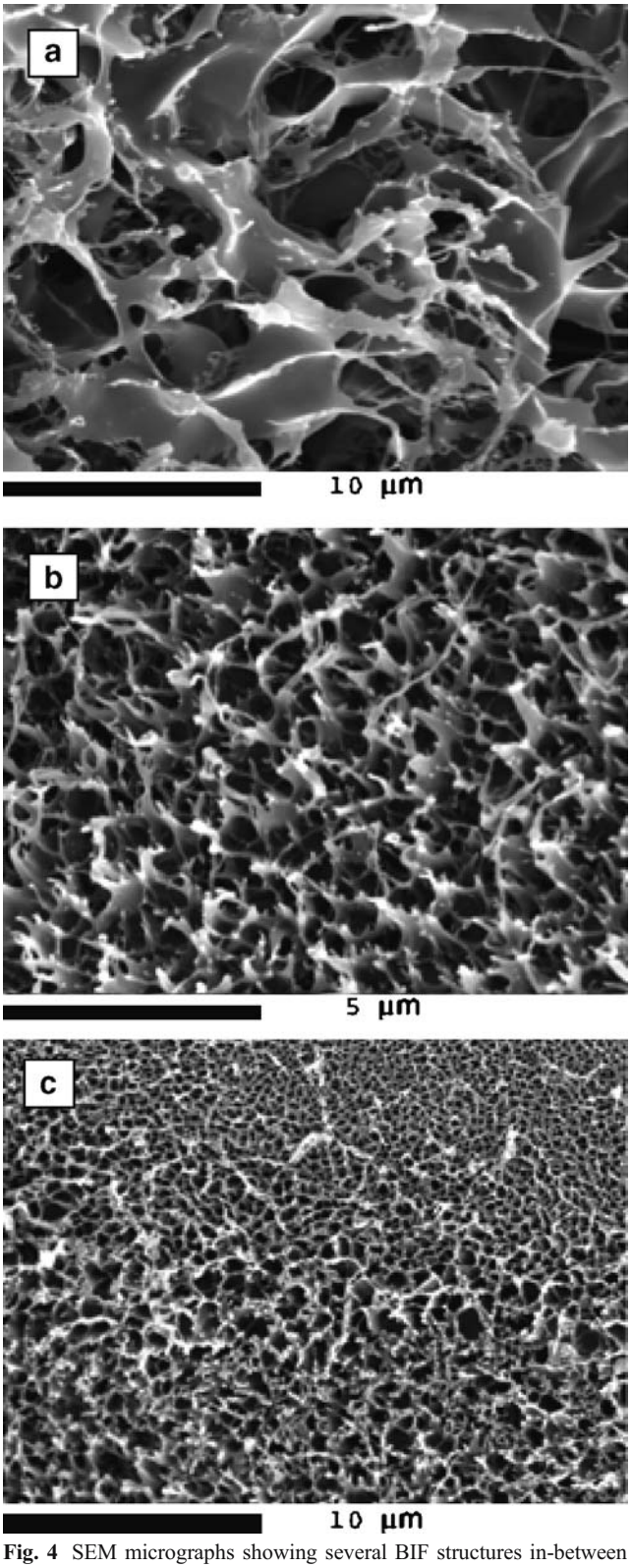

Fig. 4 SEM micrographs showing several BIF structures in-between FN and HC. **a** h-PDMAA(9.7)0.06 freeze dried from benzene, **b** and **c** h-PDMAA(4.8)0.24 freeze dried from benzene

$M_C = \rho_2/\nu_e = 7.1 \times 10^4$ *g/mol* and the corresponding radius of gyration is R_g=7 nm (estimated as in reference [17]), about one tenth of the filament thickness. For uncrosslinked PDMAA coils, R_g=40 nm for $M_n = 3 \times 10^6$ [17], and thus, the filament thickness is about 25 times R_g. Hence, only a few chains between crosslinks might form the section of filaments in the FN of hydrogels, whereas the number of entangled coils that might be found in the section of FN of l-PDMAA swollen in benzene is about double. FN microstructures were previously observed [5] for physical gels of uncrosslinked synthetic polymers and biopolymers. Figure 3c looks similar to particulate gels formed by compact globules that aggregate into random clumps and chains to give a continuous network whose fibrils have approximately the width of the original globule.

BIF structures are mainly observed in samples that were synthesized with low crosslinker ratio in the feeding (Fig. 4), and therefore, have a low crosslinking density, below 3×10^{-2} mol/L (Table 1). They seem to be the transition between FN and HC microstructures. With crosslinking densities above 3×10^{-2} mol/L, more perfect films can be formed and pure HC structures were observed. The size of holes in BIF structures are also in-between those of FN and HC microstructures (Table 2).

Figure 5 shows HC structures observed in different samples prepared both by freeze drying from benzene and by critical point drying. Film thickness is about 0.15 µm for sample h-PDMAA(4.8)0.24, which corresponds to a larger number of chains between crosslinks than for filaments of the FN. The mean Feret's diameter of the HC cells is between 0.5 (if some BIF structures close to HC are considered) and 3.5 µm, and the heterogeneity of any sample is even larger than for FN in such a way that, although average values seem to increase moderately with ν_e in Table 2, a larger set of values would be necessary to support that conclusion more strongly.

Influence of the method of preparation

FNs were observed in specimens freeze dried from benzene, both in the surface and in the bulk, in macroporous and conventional samples. Nevertheless, FNs collapse frequently in samples prepared either by critical point drying [5] or by freeze drying from water, more easily in the surface than in bulk. Honeycomb-like structures were observed by freeze drying from benzene and by the critical point drying method, in the bulk, and frequently associated to zones of fracture. Hence, the best method to observe open structures is freeze-drying of samples swollen in benzene.

Freeze drying is usually applied to samples swollen in water, the natural state of hydrogels; they are rapidly frozen in liquid nitrogen and then frozen water is removed by sublimation with high vacuum, keeping the pressure below

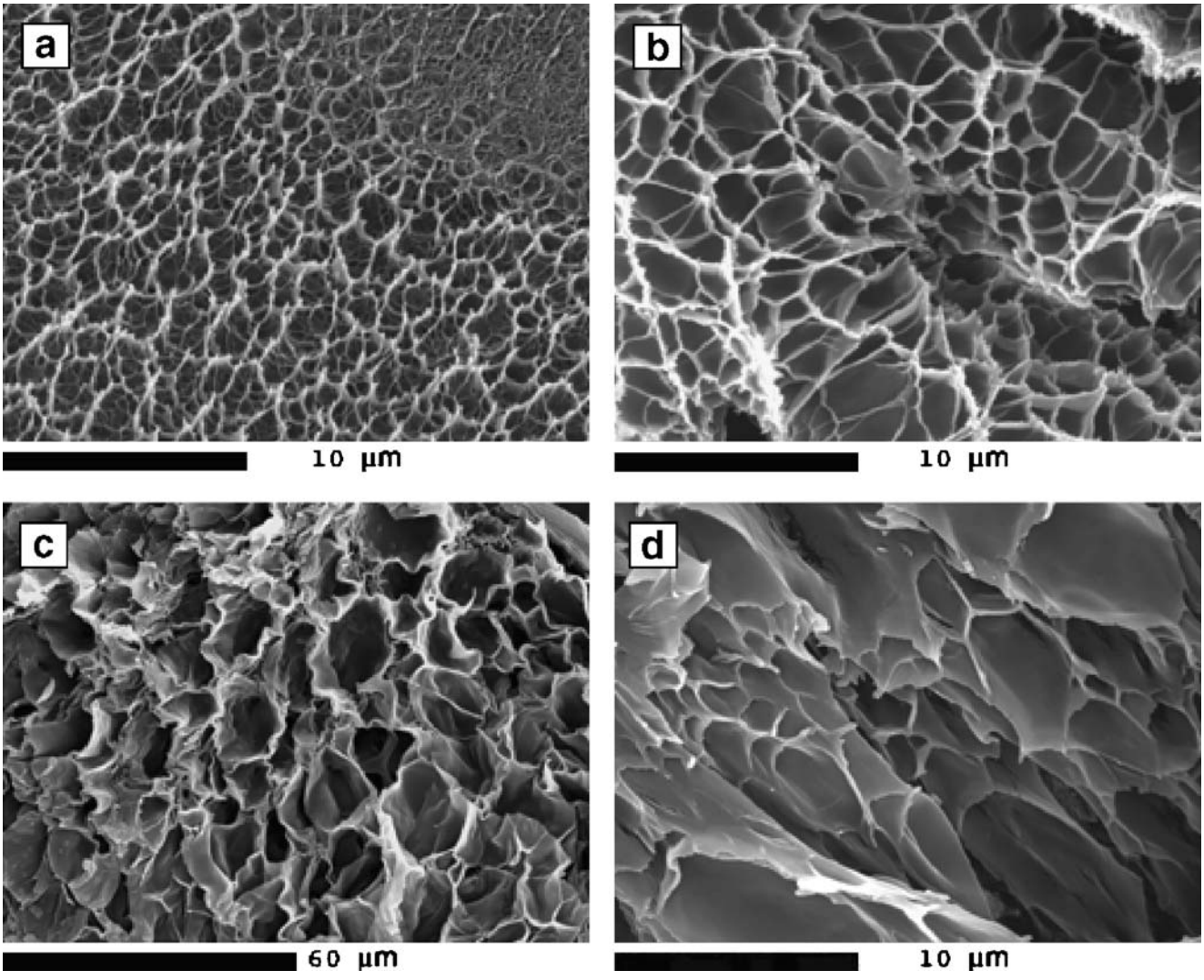

Fig. 5 SEM micrographs showing several HC structures of different cell size: **a** mh-PDMAA(9.7)0.26 freeze dried from benzene; **b** h-PDMAA (4.9)0.58 freeze dried from benzene; **c** mh-PDMAA(9.8)0.62 prepared by critical point drying; **d** h-PDMAA(4.8)0.24 prepared by critical point drying

the triple point to guarantee the direct transformation of solid in vapor, i.e., to avoid melting. Benzene has an advantage as swelling solvent, the pressure and temperature of its triple point are larger than for water [29], and therefore, it is easier to achieve the proper conditions for freeze drying. Samples prepared by freeze drying from water, as well as samples prepared by the critical point method, show, very often, collapsed structures, whereas samples prepared by freeze drying from benzene show open structures even in the surface.

However, even for samples freeze dried from benzene, some collapsed structures of different origin were observed in transparent and opaque samples. Upon drying transparent samples, it may happen that the solvent melts in some zones forming polymer domains highly compacted, without micrometric pores. Water vapor may also condense on a portion of surface, and such zones become waxy surfaces by solvent evaporation. Something similar happens by slow CO_2 extraction at the critical point: the swollen sample accommodates to progressively more concentrated domains before totally releasing the solvent, unless solvent extraction is quick enough to kinetically avoid the collapse of micropores.

Collapsed microstructures

The simplest collapsed microstructure (Fig. 8) is formed by pea-like polymer spheres. These pea-like structures may be observed in transparent samples in coexistence with open structures, placed in different zones of a single specimen or in different specimens prepared by different methods, and in such a case, they are likely artifacts. Nevertheless, pea-

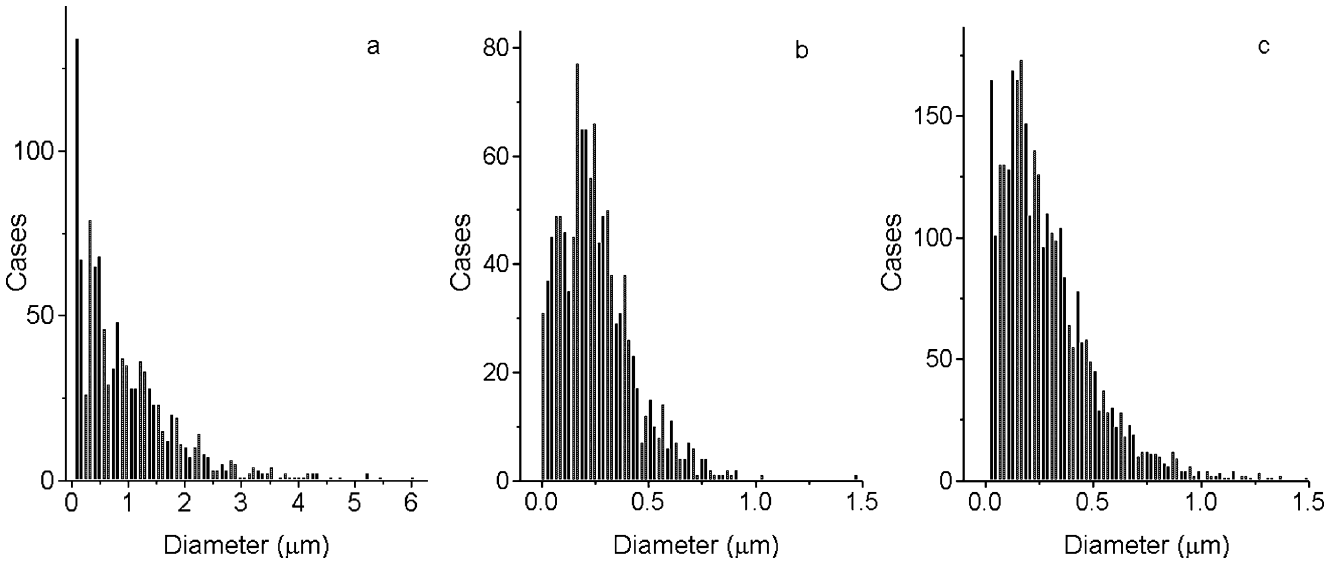

Fig. 6 Size distributions of FN holes observed for **a** l-PDMAA, **b** h-PDMAA(4.8)0.24, and **c** mh-PDMAA(9.8)0.62

like spheres of around 5 μm in diameter are the only microstructure observed for the opaque sample mh-PDMAA(9.9)2.3 in specimens prepared by different methods (Fig. 8). This sample is white and has no integrity; it breaks spontaneously into small pieces during washing. Opaque samples are expected to be formed by dense or high refractive index structures larger than the wavelength of visible light (around 0.5 μm), which reflect incident light. The large crosslinker ratio in the feeding gives place to phase separation during polymerization [15, 16] and collapsed structures are fixed in postgel reactions. Consequently, the microstructure is permanently formed by compact structures, regardless of the method of sample preparation for microscopy.

Table 2 Average diameter (D_{av}) and average width distribution (ΔD_{av}) of holes between polymer filaments (in FN) and polymer film walls (in BIF or HC) determined by analysis of SEM micrographs

Sample	D_{av} (μm)	ΔD_{av} (μm)	
l-PDMAA	1.17	1.32	FN
h-PDMAA(4.8)0.24	0.36	0.30	FN
	0.57	0.72	BIF
	1.40	2.35	HC
h-PDMAA(4.9)0.47	0.26	0.18	FN
h-PDMAA(4.9)0.52	0.21	0.15	FN
h-PDMAA(4.9)0.58	1.10	1.80	HC
h-PDMAA(4.9)1.0	0.20	0.14	FN
h-PDMAA(3.0)0.92	0.38	0.29	FN
mh-PDMAA(9.7)0.26	0.38	0.25	FN
	0.90	0.71	BIF–HC
mh-PDMAA(9.7)0.36	0.97	0.80	HC
mh-PDMAA(9.8)0.62	0.44	0.38	FN
	2.79	4.53	HC

Conclusions

This work reports on the structure in the micrometer scale of macroporous and conventional PDMAA hydrogels studied by SEM. Three types of open structures were observed: (a) filaments of a three-dimensional network, which extend to large distances with respect to the mesh size (FNs); (b) films interconnected in cells as in honeycomb networks, which extend to a smaller number of units than FN (HC); and (c) intermedium structures, which, in some zones, become FN and in others develop small and imperfect cells of HC (BIF). SEM micrographs show the micropores that were filled with solvent in the swollen state, as empty holes, totally connected in FN and compartmentalized in closed cells in HC.

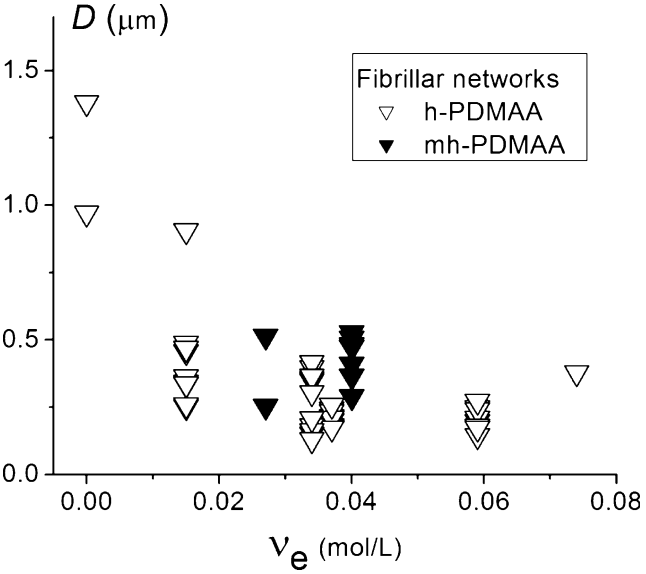

Fig. 7 Mean Feret's diameter of holes in FN micrographs obtained of uncrosslinked, macroporous, and conventional PDMAA

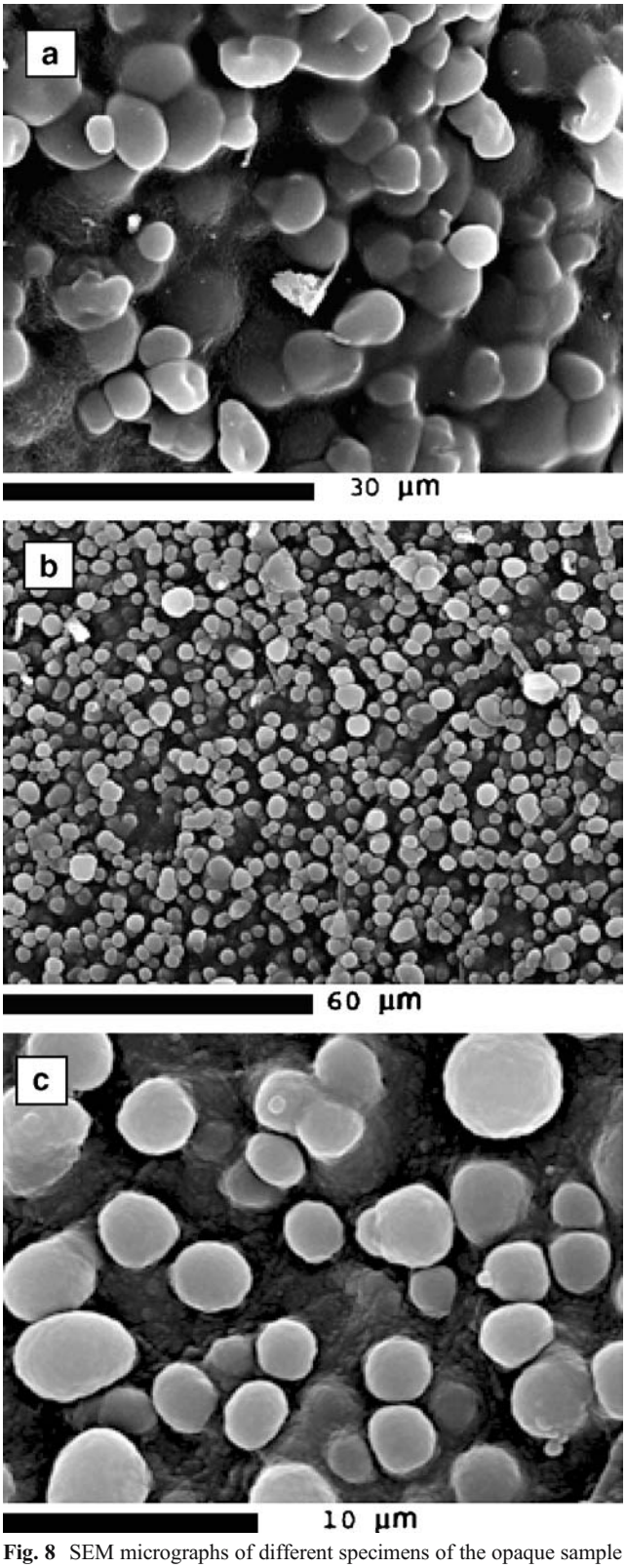

Fig. 8 SEM micrographs of different specimens of the opaque sample mh-PDMAA(9.9)2.3 obtained by freeze drying from benzene (**a**) and by critical point drying (**b**, **c**)

Image analysis of SEM micrographs allows determining the size of micropores and the thickness of polymer filaments and films. It was thus found that the size of FN, HC, or BIF structures is heterogeneous in different parts of a given specimen or in different specimens of a sample. Within that dispersion, the mesh size of FN is around 0.3 μm; it decreases with increasing crosslinking density of the sample, and macroporous and conventional gels draw the same curve. The mesh size of HC is larger, in the range of 0.5 to 3 μm. FNs were observed in practically all the samples here studied but HCs were observed only in samples with crosslinking densities above 3×10^{-2} mol/L, and below that value, BIF structures were observed instead. The uncrosslinked polymer shows only FN of large mesh size, about 1 μm.

Opaque samples have a polymer matrix intrinsically formed by collapsed structures, mainly pea-like structures, due to phase separation during polymerization. Such collapsed structures may also be observed if solvent melts or water vapor condensates in the process of drying, but they may be distinguished as artifacts if they coexist with open structures. For transparent samples, open structures were more frequently observed in specimens freeze dried from benzene, whereas the other methods (freeze drying of water-swollen samples or critical point drying) favor the formation of collapsed structures.

The glass transition temperature and the corresponding crosslinking density of the xerogels increases with the crosslinker ratio in the reacting mixture, and both the macroporous and conventional samples overimpose in a single curve. It means that the two types of gels have an equivalent structure in the nanometer scale. Hence, it may be concluded that, in spite of the very different structure of macroporous and conventional gels in the millimeter scale, they are quite the same in scales below, in the micrometer and nanometer scales. This result is particularly important in designing fast responsive gels to external stimulus. The contribution of micropores to the equilibrium swelling, to the deswelling rate, or to drug delivery should be the same both in conventional and macroporous gels, and thus, differences in their behavior should be ascribed only to macropores in the millimeter scale.

Acknowledgments This work received financial support from DGI (Spain) under grant CTQ2004-05706/BQU and from Universidad a Distancia. SEM measurements were carried out in the Centro de Microscopía Electrónica "Luis Bru" of the Universidad Complutense, Madrid. The authors wish to thank to Dr. A. Horta and Dr. L. Bailey for critical reading of the manuscript.

References

1. Serizawa T, Wakita K, Kaneko T, Akashi M (2002) J Polym Sci A Polym Chem 40:4228
2. Barbucci R, Consumi M, Magnani A (2002) Macromol Chem Phys 203:1292

3. Zhou X, Weng L, Chen Q, Zang J, Shen D, Li Z, Shao M, Xu J (2003) Polym Int 52:1153
4. Zhang XZ, Chu CC (2004) Colloid Polym Sci 282:589
5. Trieu HH, Qutubuddin S (1994) Colloid Polym Sci 272:301
6. Kato N, Takahashi F (1997) Bull Chem Soc Jpn 70:1288
7. Pastoriza A, Pacios IE, Pierola IF (2005) Polym Int 54:1205
8. Pacios IE, Horta A, Renamayor CS (2004) Macromolecules 37:4643
9. Patel VR, Amiji MM (1996) Pharm Res 13:588
10. Monleon Pradas M, Gómez Ribelles JL, Serrano Aroca A, Gallego Ferrer G, Suay Antón J, Pissis P (2001) Polymer 42:4667
11. Kishi R, Kihara H, Miura T (2004) Colloid Polym Sci 283:133
12. Apkarian RP, Wright ER, Seredyuk VA, Eustis S, Lyon LA, Conticello VP, Menger FM (2003) Microsc Microanal 9:286
13. Kellenberger E (1987) The response of biological macromolecules and supramolecular structures to the physics of specimen cryopreparation. In: Steinbrecht RA, Zierold K (eds) Cryotechniques in biological electron microscopy. Springer, Berlin Heidelberg New York
14. Reichelt R, Schmidt T, Kuckling D, Arndt KF (2004) Macromol Symp 210:501
15. Baselga J, Llorente MA, Fuentes IH, Piérola IF (1989) Eur Polym J 25:471
16. Baselga J, Llorente MA, Nieto JL, Fuentes IH, Piérola IF (1988) Eur Polym J 24:161
17. Pacios IE, Lindman B, Horta A, Thuresson K, Renamayor CS (2002) Colloid Polym Sci 280:517
18. Trossarelli L, Meirone M (1962) J Polym Sci 23:445
19. Abramoff MD, Magelhaes PJ, Ram SJ (2004) J Biophoton Int 11 (7):36–42
20. Flory PJ (1953) Principles of polymer chemistry. Cornell University Press, Ithaca, NY
21. Bershtein VA, Egorov VM (1994) Differential scanning calorimetry of polymers. Ellis Horwood, New York
22. Pacios IE, Pierola IF (2006) Macromolecules 39:4120
23. Alves NM, Gómez-Ribelles JL, Mano JF (2005) Polymer 46:491
24. DiMarzio EA (1964) J Res Natl Bur Stand A Phys Chem 68:611
25. Monleon-Pradas M, Gómez-Rivelles JL, Serrano-Aroca A, Gallego-Ferrer G, Suay-Antón J, Pissis P (2001) Colloid Polym Sci 279:323
26. Zhang XZ, Wu DQ, Chu CC (2004) Biomaterials 25:3793
27. Yoshinobu M, Morita M, Higuchi M, Sakata I (1994) J Appl Polym Sci 53:1203
28. Maia J, Ferreira L, Carvalho R, Ramos MA, Gil MH (2005) Polymer 46:9604
29. Riddick JA, Bunger WB, Sakano TK (1986) Organic solvents. Physical properties and methods of purification, 4th edn. Wiley-Interscience, New York